Tethered capsule *en face* optical coherence tomography for imaging Barrett's esophagus in unsedated patients

Kaicheng Liang, Osman O. Ahsen, Annalee Murphy, Jason Zhang, Tan H. Nguyen, Benjamin M. Potsaid, Marisa Figueiredo, Qin Huang, Hiroshi Mashimo, James G. Fujimoto

Supplementary Information

OCT features of dysplasia

Tethered capsule OCT enables wide field imaging and can potentially identify focal regions of dysplasia in non-dysplastic Barrett's esophagus (NDBE). Here, we present preliminary findings on candidate features for dysplasia which could be used for future study design. In addition, if tethered capsule OCT is used for screening, findings suggestive of dysplasia could be used to inform follow up endoscopy/biopsy, directing biopsies to suspicious regions or indicating a denser biopsy sampling than the standard Seattle protocol.

Methods

The tethered capsule OCT datasets were assessed by an expert reader (KCL) for candidate features of dysplasia. The reader was unblinded to patient history and endoscopic findings in order to identify distinctive image features/traits associated with clinical history and biopsy histology. Two candidate features were identified and assessed: atypical gland clusters (AGCs)[1] and irregular mucosal patterns (IMPs)[2]. AGCs were defined as atypical glands, including non-elliptical shape, branching or internal debris, with a clustered density of >5 atypical glands appearing over the depth of BE in a 5 mm square (25 mm^2) *en face* area, observable

in *en face* images down to ~1 mm deep in BE mucosa. The *en face* density criteria for atypical glands were added to previous cross-sectional criteria[1], in accordance with previous *en face* OCT studies[2]. The 5 mm square area criterion was chosen as a threshold based on assessment of the image data because glands distributed over a larger area in *en face* images appeared to be unassociated. Adjacent areas that had >5 atypical glands were recorded as a single clustered region. The 1 mm depth range was chosen to encompass the boundary of lamina propria and muscularis mucosa. AGCs were assessed using simultaneous 'orthoplane' viewing of the *en face* and cross-sectional image series. *En face* IMPs were defined following recent *en face* OCT studies[2] and using criteria similar to narrowband imaging (NBI)[3], including distortion/absence of mucosal patterns. The two features were assessed separately and demarcated in the *en face* images. The features were counted to determine the absolute occurrence rate (occurrences/patient), per-area occurrence rate (occurrences/approximate contacted area), and occurrence rate of IMP with underlying AGC. Features which occurred in BE near (within 1 cm of the GEJ) were noted.

Results

Supplementary Figure 1 and Video 1 shows representative results from a treatment naïve patient referred for treatment for prior histological LGD diagnosis. The area imaged (Figure 1A) was ~4 cm (capsule circumference) x ~9 cm (approximate pullback length). The mean tissue contact over the BE segment was 98%. The capsule moved slower/faster than the tether pullback over some regions, resulting in a stretched/compressed appearance because the *en face* image is displayed versus time, rather than the actual longitudinal distance travelled by the

capsule. Despite these artifacts, features in the *en face* images are distorted only in the longitudinal direction and can be interpreted by experienced readers.

AGCs (Figure 1B-C) were observed in the *en face* images. A contrast enhanced, full depth projection *en face* OCT image (Figure 1D) was used to visualize regions of regular mucosal patterns (Figure 1G), IMPs (Figure 1E-F), and absence of pattern (interpreted as irregular) (Figure 1H). Some IMPs had underlying AGCs. Cross-sectional images also showed atypical glands (Figure 1I-J), as well as features such as surface signal > subsurface (Figure 1K), and normal columnar epithelium (Figure 1L).

Supplementary Table 1 and Figure 2 summarize the features observed in the patient cohorts (history of NDBE vs dysplasia/treatment). The occurrence rates of IMPs, AGCs, and overlapping (combined) features are reported on a per-patient and per-area basis. In the neoplasia cohort, IMPs with underlying AGCs had 1.7 occurrences/patient and 0.36 occurrences/area, while in the NDBE cohort there were only 0.22 occurrences/patient and 0.01 occurrences/area.

The occurrence rate for the NDBE cohort is reported by patient history at the time of imaging, noting that 2/9 patients in the NDBE cohort each had a single occurrence of IMP with underlying AGC; standard endoscopic Seattle protocol of 4-quadrant biopsies obtained from the longitudinal position closest to the observed features showed LGD in one patient and indefinite dysplasia in the second patient. Thus, the rate of IMP with underlying AGC in the 7 patients with true NDBE status was zero occurrences/patient. These results suggest a strong association of IMP and underlying AGC with neoplasia, albeit in a small study cohort.

Discussion

The occurrence rates of IMPs and AGCs in this study were associated with neoplasia status and treatment history. IMPs with underlying AGCs occurred more frequently in treatment naïve neoplasia patients (3/3 patients, 3.0 occurrences/patient, 0.31/area) than in the treated neoplasia cohort (2/4 patients, 0.75 occurrences/patient, 0.40/area). 2/9 patients in the history of NDBE cohort had no endoscopically visible lesions and received only Seattle protocol, but OCT imaging revealed IMPs with underlying AGCs. These patients were subsequently found to have LGD and indefinite dysplasia on 4-quadrant biopsies from the approximate longitudinal position of these OCT features. The remaining 7 patients with NDBE history did not have IMPs with underlying AGCs and did not have dysplasia on Seattle protocol biopsy. These findings suggest that IMPs with underlying AGCs are a candidate marker for dysplasia and elevated risk.

These results are consistent with a previous endoscopic study using micromotor OCT catheter probes with biopsy or endoscopic mucosal resection (EMR) histology from the OCT imaged region[2]. Micromotor catheter probes image a small (~10 mm x 16 mm) field of view compared to the tethered capsule (~4 cm x 10 cm). However, this previous study allowed spatially correlated biopsy/resection using a dual channel endoscope. Blinded reading of 74 OCT datasets with correlated histology (49 NDBE, 25 neoplasia) from 44 patients identified atypical glands under IMPs in 75% of neoplasia (96% of treatment naïve neoplasia) vs. 30% of NDBE (43% of short and 18% of long segment NDBE)[2].

Atypical glands can be assessed using either *en face* or cross-sectional views, but the extent and organization of clustering are more readily appreciated in *en face* views. Atypical glands are associated with neoplasia, but also occur in NDBE, reducing specificity for this feature[4]. The present study showed AGCs occurred at

rates of 3.0/patient and 0.60/area in neoplasia, versus 1.3/patient and 0.30/area in patients with NDBE history. A multi-center study of NBI criteria for dysplasia based on *en face* features including IMPs showed 80% sensitivity and 88% specificity[3]. Either AGCs or IMPs can have substantial independent occurrences, but their combination (AGC under IMP) may have a sensitive and more specific association with neoplasia. The combination of OCT atypical gland criteria with *en face* IMPs from either NBI or OCT may improve the detection of neoplasia vs NDBE.

A substantial fraction of features in all cohorts occurred near the GEJ (Supplementary Table 1), a region reported to have low OCT feature specificity[2 , 5]. Glands in the proximal cardia may be mistaken for atypical glands near the GEJ, resulting in over counting and false positives[6]. The role of cardiac mucosa at the GEJ is debated, and it has been proposed that GEJ glands may progress to BE and have pre-malignant potential[7]. The large field of view and *en face* visualization provided by tethered capsules may improve GEJ assessment compared to slower cross-sectional OCT balloon imaging and elucidate the pathogenesis of BE and dysplasia originating from GEJ features. Treated patients appeared to have higher rates of IMPs and AGCs. This finding might be associated with the ablation procedure, however, these patients had short residual BE lengths after prior treatment; therefore the majority of features were near the GEJ, where glands in the proximal cardia might be mistaken for AGCs.

Limitations of this analysis include the small patient enrollment, which necessitated the use of an unblinded OCT expert to interpret the data while cognizant of patient history. Another limitation was the lack of histological correlation with OCT features as noted in the manuscript.

If direct correlation of OCT image features and biopsy is not technically feasible, one would perform a larger study enrolling patients with gastroesophageal reflux disease (GERD) to evaluate the tethered capsule for screening and risk stratification. Patients with suspected BE on capsule imaging would have follow up endoscopy and biopsy, then the association and sensitivity/specificity between capsule imaging and follow up endoscopy/biopsy would be assessed. Similarly, if a patient had features suggesting dysplasia on capsule imaging, they would have follow up endoscopy with enhanced biopsy sampling and the association between capsule imaging and biopsy histology would be assessed. This latter study would require including patients with history of dysplasia because rates of dysplasia are very low in a typical screening population.

OCT features in patient subgroups	All neoplasia (n=7)	Treatment naïve neoplasia (n=3)	Ablated neoplasia (n=4)†	History of NDBE (n=9)	NDBE (n=7) ††
Irregular mucosal patterns (all)					
No. of patients	6/7	3/3	3/4	6/9	4/7
Occurrences	17 (2.4/pt)	11 (3.7/pt)	6 (1.5/pt)	10 (1.1/pt)	8 (1.1/pt)
>1cm from GEJ	3 (0.43/pt)	2 (0.67/pt)	1 (0.25/pt)	7 (0.77/pt)	5 (0.71/pt)
Occurrences per cm^2 area*	0.56	0.40	0.72	0.06	0.05
Irregular mucosal patterns w/ atypical gland clusters					
No. of patients	5/7	3/3	2/4	2/9††	0/7
Occurrences	12 (1.7/pt)	9 (3.0/pt)	3 (0.75/pt)	2 (0.22/pt)	0 (0/pt)
>1cm from GEJ	3 (0.43/pt)	2 (0.67/pt)	1 (0.25/pt)	2 (0.22/pt)	0 (0/pt)
Occurrences per cm^2 area	0.36	0.31	0.40	0.008	0
Atypical gland clusters (all)					
No. of patients	7/7	3/3	4/4	7/9	5/7
Occurrences	21 (3.0/pt)	11 (3.7/pt)	10 (2.5/pt)	12 (1.3/pt)	10 (1.4/pt)
>1cm from GEJ	6 (0.86/pt)	4 (1.3/pt)	2 (0.5/pt)	6 (0.67/pt)	4 (0.57/pt)
Occurrences per cm^2 area	0.60	0.40	0.81	0.30	0.38

*Mean of occurrences/area for each patient, where total area per patient is approximated by BE maximal extent × capsule circumference × fraction of BE area in contact.

†One patient out of 4 had no visible BE on endoscopy and was thus excluded from the mean occurrences/area computation. Features observed at the GEJ were counted as occurrences.

††The two patients with a history of NDBE having irregular mucosal patterns with underlying atypical gland clusters had biopsies with low-grade dysplasia and indefinite for dysplasia. This column reflects true NDBE status at the time of imaging.

Supplementary Table 1. Occurrence rates of OCT features in BE, irregular mucosal patterns, atypical gland clusters, and irregular mucosal patterns with underlying atypical gland clusters in patient subgroups.

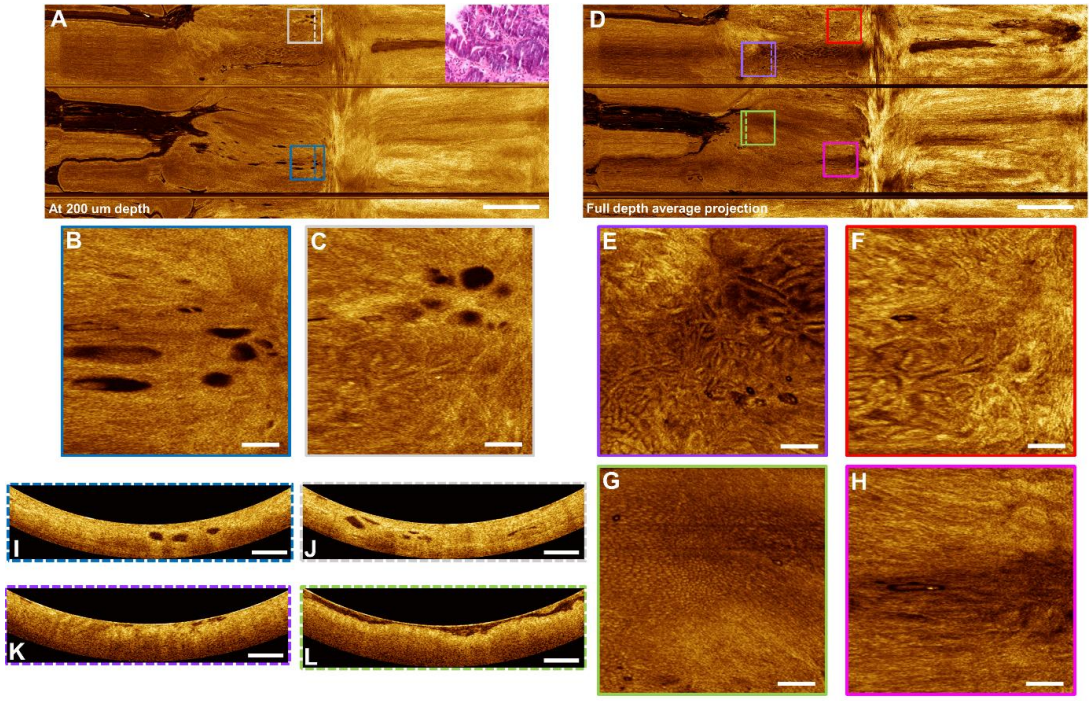

Supplementary Figure 1. Tethered capsule volumetric OCT from a patient with C0.5M2 and treatment naïve low-grade (basal crypt) dysplasia with biopsy (inset) from previous EGD. *En face* OCT image (A) at 200 um depth from surface, averaged over 80 um depth range (200 um to 280 um), showing dilated glands and (D) *en face* image averaged over ~1 mm depth range (full projection) for contrast enhancement of mucosal pattern. Scale bar 1 cm. (B, C) Atypical gland clusters. (E, F) Irregular mucosal pattern. (G) Regular mucosal pattern. (H) Absence of mucosal pattern, interpreted as irregular. (I-L) Cross-sectional images co-registered to *en face* regions of interest. (I) Shows 3 dilated glands with atypical shape, but does not show the substantial clustering of >5 glands seen in the *en face* image. (K) Shows surface signal higher than subsurface, but does not show the mucosal pattern irregularity seen in the *en face* image. (L) Shows loose contact at the gastroesophageal junction,

which may confound differentiation between gastric and BE tissue. All other scale bars 1 mm.

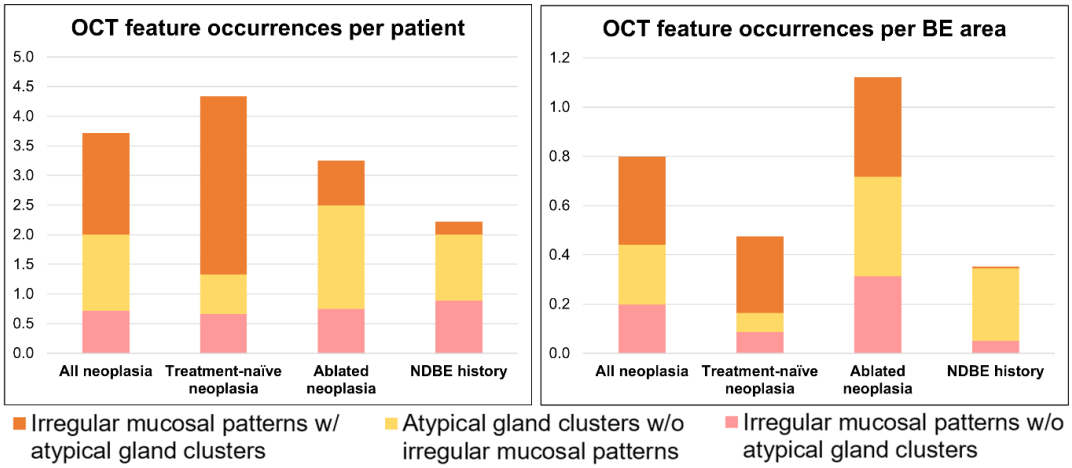

Supplementary Figure 2. Stacked bar charts of OCT feature occurrences per patient and per cm^2 of BE area. The features are plotted to avoid repeat counting, such that the stacked height indicates the total feature count. Neoplasia patients had a high occurrence rate of irregular mucosal patterns with underlying atypical gland clusters, while patients with history of NDBE showed a much lower occurrence rate. Atypical gland clusters were numerous in all subgroups and associated with a proximity to the GEJ (Supplementary Table 1).

Supplementary Video 1: Demonstration of orthoplane viewing of *en face* and cross-sectional OCT image series, using dataset presented in Supplementary Figure 1. Ultrahigh-speed tethered capsules acquire 1,000,000 A-scans per second with 300 images/second at a pullback speed of ~1 cm/second. Ultrahigh speed is important for *en face* OCT because each pixel in the *en face* view requires one A-scan. Orthoplane viewing is similar to CT reading and enables rapid and comprehensive assessment of features.

References

1. Leggett CL, Gorospe EC, Chan DK, et al. Comparative diagnostic performance of volumetric laser endomicroscopy and confocal laser endomicroscopy in the detection of dysplasia associated with Barrett's esophagus. *Gastrointestinal Endoscopy* 2016;83(5):880-88.e2.
2. Ahsen OO, Liang K, Lee H-C, et al. Assessment of Barrett's esophagus and dysplasia with ultrahigh-speed volumetric en face and cross-sectional optical coherence tomography. *Endoscopy* 2018.
3. Sharma P, Bergman JJGHM, Goda K, et al. Development and Validation of a Classification System to Identify High-Grade Dysplasia and Esophageal Adenocarcinoma in Barrett's Esophagus Using Narrow-Band Imaging. *Gastroenterology* 2016;150(3):591-98.
4. Swager A-F, Tearney GJ, Leggett CL, et al. Identification of volumetric laser endomicroscopy features predictive for early neoplasia in Barrett's esophagus using high-quality histological correlation. *Gastrointestinal Endoscopy* 2017;85(5):918-26.e7.
5. Gupta N, Siddiqui U, Waxman I, et al. Use of volumetric laser endomicroscopy for dysplasia detection at the gastroesophageal junction and gastric cardia. *World journal of gastrointestinal endoscopy* 2017;9(7):319-26.
6. Trindade AJ, Raphael KL, Inamdar S, et al. Volumetric laser endomicroscopy features of dysplasia at the gastric cardia in Barrett's oesophagus: results from an observational cohort study. *BMJ Open Gastroenterology* 2019;6(1):e000340.
7. McDonald SAC, Lavery D, Wright NA, et al. Barrett oesophagus: lessons on its origins from the lesion itself. *Nature Reviews Gastroenterology & Hepatology* 2014;12:50.